Intermediate metastable structure of the C{111}/(1×1)H-C{111}/(2×1) surface phase transition

Leonid V. Zhigilei, Deepak Srivastava, and Barbara J. Garrison
152 Davey Laboratory, Department of Chemistry, The Pennsylvania State University, University Park, Pennsylvania 16802
(Received 7 March 1996)

The pathway of the {111} diamond surface transformation between the (2×1) π-bonded chain and the (1×1) bulk-terminated structures is investigated using the molecular-dynamics technique. The metastable surface structure that mediates the H adsorption-induced phase transition from the (2×1) to the (1×1) surface reconstruction, and the crucial role played by hydrogen in the stabilization of this intermediate structure, are proposed. Atomic configurations formed by adjacent CH bonds on the mostly (2×1) structure are responsible for the energy barrier separating the metastable phase from the hydrogen-terminated (1×1) structure. Calculated vibrational spectra for the various surface reconstructions are correlated with experimental observations of Chin *et al.* [Phys. Rev. B **45**, 1522 (1992)]. The occurrence of the additional higher-frequency metastable peak, its intensity variation during hydrogen absorption, and possible reasons for the irreversible character of the surface transition are discussed based on the results of the molecular-dynamics simulation. [S0163-1829(97)01604-4]

I. INTRODUCTION

Significant technological advances made in the chemical vapor deposition (CVD) of diamond films have attracted attention to the studies of hydrogen-covered diamond surfaces. Hydrogen facilitates diamond growth by promoting sp^3 bonding, creating radical and/or reactive sites, and removing graphitic regions.[1–3] The extensive experimental and theoretical efforts undertaken during the last decade have led to significant progress in understanding the microscopic mechanisms of CVD diamond growth.[1–5] The precise role of hydrogen in the stability and growth of the various diamond surfaces, however, is not yet clear. One example of the complexity of the interaction of H atoms with carbon surfaces is the unknown mechanism of the (2×1) to (1×1) phase transformation induced by hydrogen adsorption on a diamond {111} surface (C{111}) along with the structure of an intermediate metastable surface reconstruction that appears in the initial stages of hydrogen absorption on the (2×1) π-bonded structure.[6,7]

It is generally accepted that at complete or near complete hydrogen coverage the C{111} surface is a bulk-terminated (1×1) structure, with the dangling bonds or radicals terminated by hydrogen atoms, denoted *C*{111}/(1×1)H [Fig. 1(g)]. The observed (2×1) reconstruction of the clean surface is a π-bonded chain structure, denoted C{111}/(2×1) [Fig 1(c)]. Here the radicals that would be found on the clean bulk-terminated surface are eliminated in favor of chains of sp^2-hybridized carbon atoms.[3,7–9] The structure of the C{111} surface at intermediate H coverages and the mechanisms and driving forces of surface transformation under hydrogen exposure and thermal treatment, however, are less clear. Electron-stimulated desorption mass spectroscopy experiments show that continued annealing even after complete hydrogen desorption is required for the (1×1)→(2×1) reconstruction.[9] This is also consistent with a conclusion from recent tight-binding simulations that the bulk-terminated surface does not spontaneously reconstruct to a (2×1) structure.[10,11] On the other hand, results of low-energy electron-diffraction and optical spectroscopy experiments indicate that adsorption of only a few percent of a monolayer of hydrogen is sufficient to induce the (2×1)→(1×1) phase transition.[6,12] Thus, not only are the mechanisms of transformation unknown, but they also appear to be different in the two directions.

Recent infrared-visible sum-frequency generation experiments[6,7] add more insight into the C{111} surface structural transformations resulting from hydrogen dosing and thermal annealing. The spectrum of the bulk-terminated C{111}/(1×1)H surface has a single peak at 2338 cm^{-1}. During hydrogen adsorption on the clean C{111}/(2×1) surface, it is found that an additional peak at ~2865 cm^{-1} arises in the vibrational spectrum at low H coverages. This peak is attributed to an intermediate metastable structure resulting from a hydrogen-absorption-induced phase transition from the clean (2×1) structure to the bulk-terminated (1×1)H structure.[6,13] As the hydrogen coverage increases, the intensity of the peak at ~2865 cm^{-1} initially increases, reaching its maximum value at about a half-monolayer coverage, and then gradually disappears in favor of the main peak at 2838 cm^{-1}, which is characteristic of the C{111}/(1×1)H surface. The strength of the 2865-cm^{-1} peak could be also transferred to the 2838-cm^{-1} peak by annealing the surface at about 1000 K. It is interesting that once the (1×1) surface has been annealed, the 2865-cm^{-1} peak does not appear again with any further desorption and readsorption of hydrogen. Although these results have been discussed,[10,13] the intermediate metastable structure and the reasons for the asymmetry of the structural transformations during hydrogen absorption on a C{111} surface remain unknown.

In the present work, the atomic-scale details of the role of hydrogen in the surface reconstruction are investigated using the molecular-dynamics (MD) method.[14,15] The Brenner em-

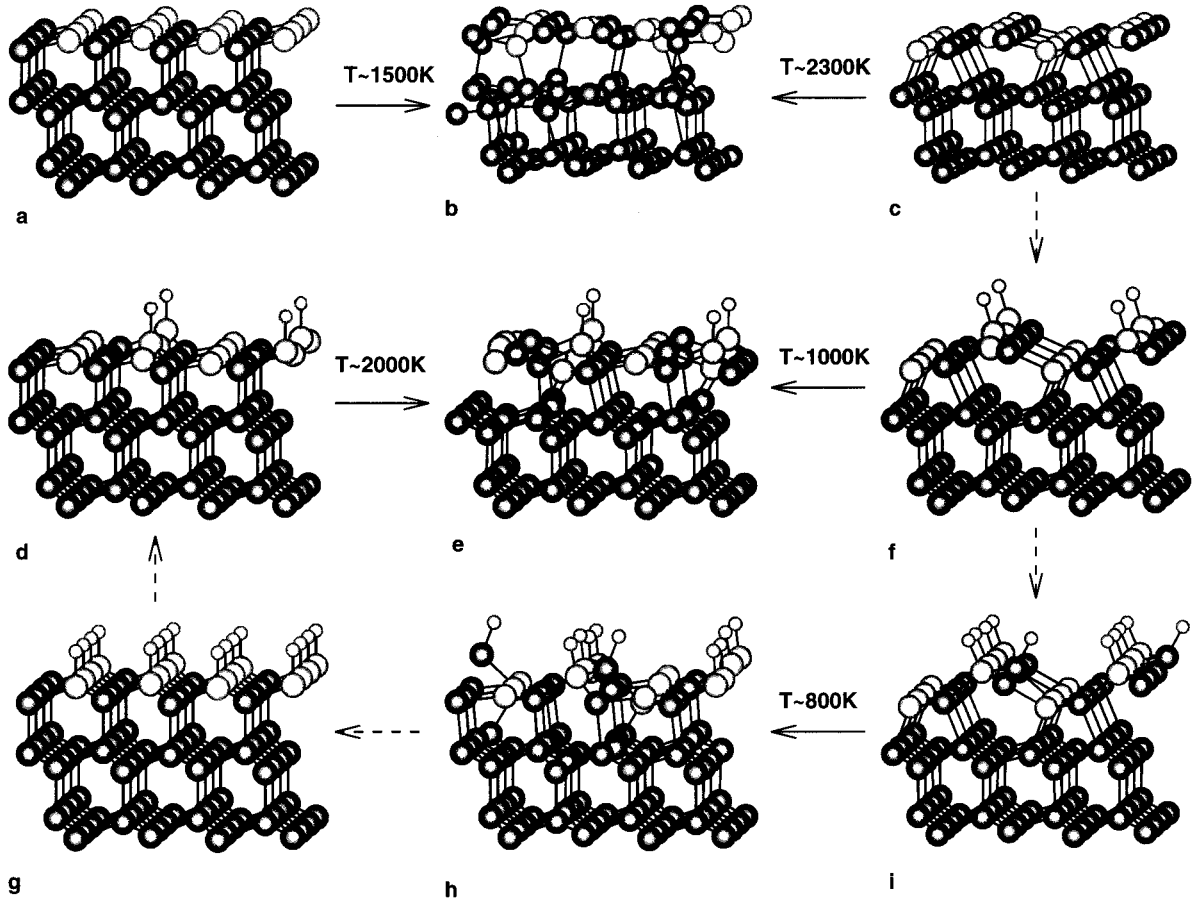

FIG. 1. Side views of various C{111} surfaces. The larger dark and light spheres represent C atoms, and the smaller spheres represent H atoms. The light C atoms are radical sites in the bulk-terminated (1×1) structure. Only the top layers of the computational cell used in the simulations are shown. The left column of structures are all bulk terminated, and the right column of structures are all π-bonded chain reconstructions. The middle column is the structures resulting from MD simulations. The different structures have different number of *H* atoms adsorbed [(a), (b), and (c)], 0%; (d), (e), and (f), 25%; (h) and (i), 62.5%, and (g), 100% of full coverage]. The solid arrows show the paths of structural transformations observed in the computer simulations. The dashed arrows show the transformations that include the H atoms migration, adsorption, or desorption and are not the subjects of simulation in the present work.

pirical reactive potential[16,17] is used to describe the interatomic interactions. This makes it possible to perform MD simulations involving structural transformations toward local-energy-minimum configurations for various hydrogen coverages. The vibrational spectra for the proposed metastable surface configuration at partial H coverage and for the bulk-terminated surface at full H coverage are calculated, and the results are correlated with the experimental infrared data. Subsequent detailed analysis of the atomic configurations together with atomistically resolved spectra calculations allow us to propose a relationship between the features of the spectra and inhomogeneous nature of the metastable surface reconstruction.

II. COMPUTATIONAL METHOD

The goal in the MD simulations is to investigate the structural rearrangements of the C{111} surface induced by the thermal treatment at various H coverages. The molecular-dynamics computational cell is composed of carbon atoms arranged in a diamond lattice that is 12 layers thick, with 16 atoms per layer. Periodic boundary conditions in the two directions parallel to the surface are imposed. In order to model different H coverages, up to 16 H atoms are attached to the top-layer carbon atoms. The top four layers of C atoms and all H atoms experience only the forces due to the appropriate potential function. The next six layers experience both the forces due to the interaction potential, as well as friction and stochastic forces via the generalized Langevin equation (GLE) method for maintaining a desired temperature.[18] The bottom two layers are held rigid and a variable time-step Nordsieck predictor-corrector is used to integrate the equations of motion.[19]

An analytic empirical potential function developed by Brenner and co-workers[16,17] is used to study the dynamics of surface structural transformations and to obtain structures corresponding to the energy minima for different hydrogen coverages. This potential function was developed to model diamond surface reactions, during which bonds can be broken and new bonds can be formed. It has been shown that the Brenner potential provides a reasonable description of surface reconstructions.[16–18] Of relevance to this investigation is that it predicts the π-bonded chain reconstruction to be more stable than the bulk-terminated structure for clean C{111}. Conversely, for the H-terminated surface, it predicts that the

bulk-terminated surface is the more stable of the two configurations.

As starting atomic configurations in the present work we use partially H-terminated π-bonded chain or bulk-terminated surface structures. Representative structures are shown in Figs. 1(c), 1(f), and 1(i) and 1(a), 1(d), and 1(g), respectively. Heating of these surfaces for 30 ps at temperatures ranging from 800 to 2300 K, and subsequent quenching to 0 K, gave us a number of trial metastable structures, including those shown in Figs. 1(b), 1(e), and 1(h).

The atomic configurations obtained from structural simulations are used as input data for the calculation of the vibrational spectra. The calculation of the vibrational spectra follows the semiclassical approach, where the initial excitation of CH bonds precedes the analysis of vibrational dynamics.[20–24] In the present calculation a quantum of energy equivalent to the zero-point energy of the stretching mode was deposited in each CH bond.[24] After excitation, a trajectory of 20 ps, was performed and the velocities, $\nu(t)$, of the H atoms saved for analysis. The generalized vibrational spectra are computed by taking the Fourier transform of the velocity-velocity autocorrelation function according to

$$I(\omega) \sim \int dt\ \exp(-i\omega t)\langle \nu_i(\tau)^* \nu_i(\tau+t)\rangle_{i,\tau},$$

where the brackets indicate averaging of the correlation function over trajectories of different H atoms i and starting times τ. In this formulation a vibrational spectrum for some specific subset of particles can be calculated by taking trajectories of only the particles of interest. Thus the correlation of spectral features with inhomogeneity in a local chemical environment can be obtained.

As have been found in the studies of the H-covered silicon surfaces,[21–23] the employment of the semiclassical approach is essential for the simulation of realistic vibrational spectra. An important prerequisite in this case is the condition that the energy deposited in the stretching mode remains in the mode during the simulation. This is not a problem in the simulation for the hydrogen-covered silicon surfaces, where the lifetimes of the SiH stretching modes are on the order of nanoseconds,[22,23,25] because the SiH stretching modes are well separated from the SiSiH bending and surface phonon modes. For the C{111}/(1×1)H surface, however, the separation of the CH stretching mode from a strong low-order resonance[24,26] with an overtone of a CCH bending mode is rather small. This results in high sensitivity of the lifetime of excited CH stretching states to slight changes in the parametrization of interatomic interactions.[24,26] Moreover, high-amplitude vibrations corresponding to the excited states of the CH stretching mode lead to the increasing importance of the anharmonic terms of the CH stretching potential function. These considerations are taken into account in deciding on an interatomic potential that is used in vibrational spectra calculations. A molecular mechanics potential in the form proposed by Allinger, Yuh, and Lii[27] ($MM3$) is employed to describe the diamond C-C interactions and the bending force constant for the CCH angles. The CH bond stretching potential is described by the function derived in *ab initio* calculation of Zhu and Louie,[13] who were particularly interested in the anharmonicity of the CH stretching mode. Furthermore, to compare well with the experimental values of the frequency of the CCH bending mode and Debye frequency, all the CC interaction force constants as well as the CCH bending force constant have been scaled down by 15%. A detailed discussion of the applicability of the $MM3$ potential to the analysis of the vibrational properties of different diamond surfaces is presented elsewhere.[24]

III. RESULTS AND DISCUSSION

MD simulations are performed to determine the role of hydrogen in the formation and stabilization of the metastable surface reconstructions in the phase transition from the C{111}/(2×1) surface to the C{111}/(1×1)H surface. In addition, we analyze the vibrational spectra associated with a possible intermediate structure, and compare it with experimental spectra.

The reconfiguration which the C{111} surface undergoes in transforming between the bulk-terminated structure [Figs. 1(a), 1(d), and 1(g)] and the π-bonded chain reconstruction [Figs. 1(c), 1(f), and 1(i)] undoubtedly involves a rather complicated rearrangement of bonds. Recent experimental studies have shown that a metastable surface structure intermediate between the (1×1) and (2×1) structures might exist in the initial stages of hydrogen absorption on the π-bonded chain surface.[6] In order to reveal the path that the surface follows during reconstruction, and the atomic-scale structure of the proposed intermediate structure, MD studies of surfaces with different hydrogen coverages are performed.

We start with hydrogen-free surfaces. The heating of the π-bonded chain reconstructed surface, up to 2300 K, results in the breaking of bonds between the first and the second double layers and formation of graphite sheet [Figs. 1(c) →1(b)]. This agrees with the recent *ab initio* MD simulation results.[28]

A similar process is observed for the hydrogen-free bulk-terminated surface at a lower temperature of 1500 K [Figs. 1(a)→1(b)]. Although this observation is not surprising once the simulation temperature is in the range of graphitization temperature,[1,2] it is not consistent with the fact that the (1×1)→(2×1) reconstruction occurs upon annealing of the C{111} surface at about 1300 K.[1–3,7,9,12,29] One possible explanation of this result is that the short-ranged character of the Brenner potential does not provide sufficient attraction to form bonds to make the five- and seven-membered rings.[18] Recent results of tight-binding simulations,[11] where the interatomic interaction is not restricted to within short range, however, also suggest that upon heating the bulk-terminated hydrogen-free surface undergoes graphitization rather than reconstruction to the π-bonded chain structure. On the basis of this observation, the existence of a graphitic transition state in the (1×1)→(2×1) reconstruction has been proposed.[11] On the other hand, a recent observation by Lee and Apai[29] showed that hydrogen cannot be eliminated from the {111} surface even after repeated heating to ~1473 K. This suggests that a small amount of hydrogen can play a part in stabilization of the {111} surface against graphitization.

Indeed, the results of our computer experiments indicate that hydrogen does stabilize the {111} surface against graphitization. We find that both the bulk-terminated and

π-bonded chain surface structures with 25% hydrogen coverage readily undergo partial reconstruction to similar intermediate structures upon heating. A side view of one of these structures along the chains, as seen in Fig. 1(e), exhibits a mixture of six-membered rings that are characteristic of the bulk-terminated surface [Fig. 1(d)] and five- and seven-membered rings typical of the π-bonded chain reconstruction [Fig. 1(f)]. Unlike the graphitization process [Figs. 1(c) $\rightarrow$1(b) and 1(a)$\rightarrow$1(b)], the number of four-coordinated sp^3-hybridized C atoms remains the same during this reconstruction process, as shown by the number of bonds that are retained between the first and second double layers in Figs. 1(d), 1(e), and 1(f). The Brenner potential predicts that the intermediate configuration depicted in Fig. 1(e) is lower in energy than the bulk-terminated and π-bonded chain structures, with the same hydrogen coverages, by 0.21 and 0.15 eV per surface atom, respectively.

Thus the MD simulations indicate that surface structure intermediate between the bulk-terminated and the π-bonded chain reconstructions is a combination of five-, six-, and seven-membered rings. The surface transformation into the intermediate structure is energetically favorable, and occurs readily at low-H coverages. The issue then is to explain the stability of the intermediate structure and the experimentally observed asymmetry in the $(1\times1)\leftrightarrow(2\times1)$ surface phase transitions. The surface configuration depicted in Fig. 1(e) can result from both the H desorption from a bulk-terminated surface [Figs. 1(g)$\rightarrow$1(d)$\rightarrow$1(e)] and H adsorption onto a (2×1)-reconstructed surface [Figs. 1(c) $\rightarrow$1(f)$\rightarrow$1(e)]. The structures shown in Figs. 1(d) and 1(f), however, are just examples of a number of possible hydrogen arrangements that could be formed in real adsorption or desorption processes. In order to discuss these processes in detail, let us reconsider the structures of the clean (1×1) and (2×1) surface reconstructions shown in Figs. 1(a) and 1(c), respectively. The C atoms that are surface radicals in the bulk-terminated (1×1) structure are shaded lighter on Fig. 1. Of note is that in the (2×1) structure some of the lighter atoms are sp^3 hybridized in the five-membered rings, and are presumably unreactive to H adsorption. In addition, there is no difference between the lighter and darker atoms in the seven membered rings of (2×1) structure [Fig. 1(c)]. Thus H adsorption should be equally probable on the light or dark sp^2-hybridized C atoms. Once a hydrogen atom has been adsorbed, not only does one carbon atom attain the sp^3 hybridization, but neighboring atoms in the same chain attain mixed sp^2/sp^3 character. Thus the adsorption of another hydrogen atom in the vicinity of an existing CH bond becomes energetically favorable. The calculations predict a 0.85-eV difference in energy for π-bonded chain-reconstructed surfaces with two CH bonds adjacent to each other in one case and spatially separated in another. On the other hand, we find that upon H adsorption the π-bonded chain reconstruction becomes unstable, and quick structural transformations take place even at moderate temperatures ($\sim$800 K). This transformation [e.g., as shown in Figs. 1(i) $\rightarrow$1(h) and 1(f)$\rightarrow$1(e)] includes carbon atom rebonding, and partial radical diffusion to the positions characteristic of the bulk-terminated structure (light atoms in Fig. 1). Further hydrogen deposition then leads to the sequential formation of the bulk-terminated surface structure.

To complete the $(2\times1)\rightarrow(1\times1)$ phase transition, the adsorbed H atoms must end up on only the light C atoms. In this transformation the hydrogen atoms adsorbed on the dark carbon atoms cause the formation of localized highly strained atomic configurations [Fig. 1(h)] that hamper the surface reconstruction to the bulk-terminated structure. The additional energy attributed to these configurations was found to increase with increasing hydrogen coverage up to 1.5 eV per defect at full coverage.

As an aside, there is an alternative scenario in which the H atoms adsorb to all the dark surface C atoms. Further diamond growth in the $\langle111\rangle$ direction would then lead to the formation of a stacking fault, or twin plane.[30–32] The predominance of this type of surface reconstruction during growth process may result in the formation of carbon phase alternative to diamond-hexagonal lonsdaleite.[33]

An accurate simulation of the migration of hydrogen atoms from dark C atoms to light C atoms is probably beyond the capability of both classical mechanics and this empirical potential.[18] At experimental annealing temperatures of $\sim$800 K, one can expect that the adsorbed H atoms may be quite mobile on the surface. The diffusion or desorption of a H atom adsorbed on a dark C atom would lead to the quick irreversible relaxation of the strained configuration. This removal of H atoms from the dark C atoms seems to be the rate-limiting step in the formation of the bulk-terminated surface structure. Indeed, when we chose as an initial configuration a half-H-covered π-bonded chain structure where all H atoms were attached to the light carbon atoms and heated it to 800 K, we found that the transition of the surface to the bulk-terminated structure was complete in about 30 ps.

In contrast to the $(2\times1)\rightarrow(1\times1)$ phase transition, the hydrogen-desorption-induced $(1\times1)\rightarrow(2\times1)$ phase transition would be mediated by a defect-free intermediate structure, in which H atoms are attached only to the light C atoms [e.g., Fig. 1(e)]. In the absence of adjacent CH bonds that are found to stabilize the intermediate structure in the $(2\times1)\rightarrow(1\times1)$ transition, H readsorption would easily cause backward reconstruction to the (1×1) bulk-terminated structure. This inference agrees with the experimental observation[6] that, after the (1×1) surface was annealed, the high-frequency additional peak did not appear again with further desorption and readsorption of hydrogen. Thus, in accordance with experimental observations,[6] the atomic level analysis based on the results of MD simulations suggests that the stable intermediate surface structure can appear only in the $(2\times1)\rightarrow(1\times1)$ direction of the phase transition.

Recent advances in surface vibrational spectroscopy provide *in situ* information about the diamond {111} surface reconstruction process.[6,7] The dynamical calculations of vibrational spectra give, therefore, an additional possibility for the direct correlation of the structures in Fig. 1 with the experimental data.

In Fig. 2 the CH stretching peak region of the computed vibrational spectra are presented. The resolution of the spectra is 2 cm^{-1}, due to the finite molecular-dynamics trajectory input into the fast-Fourier-transform algorithm. The single sharp peak is observed in the high-frequency region for the bulk-terminated surface at the position of 2853 cm^{-1}.

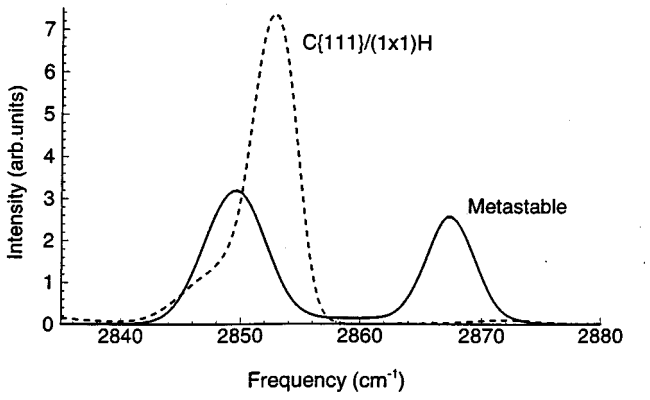

FIG. 2. Spectral intensity of the CH stretching mode calculated for the H-covered bulk-terminated and metastable partially H-covered C{111} surface reconstructions, depicted in Figs. 1(g) and 1(h), respectively.

On the other hand, the spectra of the partially covered metastable structure depicted in Fig. 1(h) has two well-defined peaks separated by 18 cm^{-1} as shown in Fig. 2. The position of the low-frequency peak closely matches the calculated position of the peak from the bulk-terminated structure. The appearance of the spectra is similar to the experimental IR spectra in which an additional peak on the high-frequency side is found for the metastable C{111} partially H-covered surface.[6]

In order to reveal the nature of the high-frequency peak, we perform atomistically resolved vibration spectral analysis. Different subsets of the hydrogen atoms are used for the velocity autocorrelation function calculations and the subsequent Fourier transforms. We find that only the atoms included in the strained configurations and responsible for the stabilization in the metastable structure contribute to the formation of the additional high-frequency peak. In contrast, the stretching vibration frequency of the CH oscillators that do not have adjacent CH neighbors corresponds to the lower frequency peak.

As it is discussed above, both annealing and high hydrogen coverage can cause H atoms to diffuse from the dark carbon atoms, resulting in the strength of the metastable peak to be transferred to the main peak which is characteristic to the bulk-terminated structure. Local rearrangement of C-C bonds following the hydrogen diffusion from the dark carbon atoms would lead to the quick relaxation of the strained configuration. Thus, because of the irreversible character of the hydrogen diffusion, the second peak does not appear again with further desorption or readsorption of hydrogen. Hence the experimental inference about unidirectional character of the surface reconstruction[6,13] can now be understood in the context of the molecular-dynamics simulation results.

IV. CONCLUSION

Molecular-dynamics simulations of diamond surface annealing together with vibrational spectra calculations yield insight into the pathway by which the {111} surface undergoes transformation between the (2×1) π-bonded chain reconstruction and the (1×1) bulk-terminated structure. We find that heating of the hydrogen-free bulk-terminated surface results in the surface graphitization rather than reconstruction to the (2×1) π-bonded chain structure. The results of the simulations suggest, however, that a small amount of hydrogen stabilizes the {111} diamond surface against graphitization, and can play an important part in the (1×1)–(2×1) surface reconstruction.

Concerning the H adsorption-induced phase transition from the (2×1) to the (1×1) surface reconstruction, we find that in the early stages of hydrogen deposition on a (2×1)-reconstructed surface atomic configurations comprised of adjacent CH bonds can be readily formed. In subsequent surface transformation, these configurations serve as localized structural defects that stabilize the metastable structure, and determine the energy barrier separating the metastable structure reconstruction from the hydrogen-terminated (1×1) structure. Vibrational spectra calculations confirm that just these strained atomic configurations are responsible for the formation of an additional metastable peak in the high-frequency region. Thermal annealing and further H dosing can cause the irreversible relaxation of these defected configurations, and hence the gradual transfer of the metastable peak strength to the peak corresponding to the (1×1) bulk-terminated surface structure occurs. On the whole, the picture derived from the computer modeling agrees well with the existing experimental data.

We gratefully acknowledge financial support from the Office of Naval Research through the Medical Free Electron Laser Program. The computational support for this work was provided by the IBM Selected University Research Program at Penn State University.

[1] *Proceedings of the 5th European Conference on Diamond, Diamond-like and Related Materials, Ciocco, Italy, 1994* [Diamond Relat. Mater. **4**, N4-6 (1995)].

[2] *Thin Film Diamond*, edited by A. Lettington and J. W. Steeds (Chapman & Hall, London, 1994).

[3] B. B. Pate, Surf. Sci. **165**, 83 (1986).

[4] S. F. Harris and D. G. Goodwin, J. Phys. Chem. **97**, 23 (1993).

[5] E. J. Dawnkaski, D. Srivastava, and B. J. Garrison, J. Chem. Phys. **102**, 9401 (1995); **104**, 5997 (1996).

[6] R. P. Chin, J. Y. Huang, Y. R. Shen, T. J. Chuang, H. Seki, and M. Buck, Phys. Rev. B **45**, 1522 (1992).

[7] R. P. Chin, J. Y. Huang, Y. R. Shen, T. J. Chuang, and H. Seki, Phys. Rev. B **52**, 5985 (1995).

[8] D. Vanderbilt and S. G. Louie, Phys. Rev. B **29**, 7099 (1984); **30**, 6118 (1984).

[9] A. V. Hamaza, G. D. Kubiak, and R. H. Stulen, Surf. Sci. Lett. **206**, L833 (1988).

[10] B. N. Davidson and W. E. Pickett, Phys. Rev. B **49**, 11 253 (1994).

[11] G. Jungnickel, Th. Frauenheim, D. Porezag, W. R. L. Lambrecht, B. Segall, and J. C. Angus, Bull. Am. Phys. Soc. **40**, 772 (1995).

[12] Y. Mitsuda, T. Yamada, T. J. Chuang, H. Seki, R. P. Chin, J. Y.

Huang, and Y. R. Shen, Surf. Sci. Lett. **257**, L633 (1991).
[13] X. Zhu and S. G. Louie, Phys. Rev. B **45**, 3940 (1992).
[14] D. W. Heermann, *Computer Simulation Methods in Theoretical Physics* (Springer-Verlag, Berlin, 1990).
[15] M. P. Allen and D. J. Tildesley, *Computer Simulation of Liquids* (Clarendon, Oxford, 1987).
[16] D. W. Brenner, Phys. Rev. B **42**, 9458 (1990).
[17] D. W. Brenner, J. A. Harrison, C. T. White, and R. J. Colton, Thin Solid Films **206**, 220 (1991).
[18] B. J. Garrison, P. B. S. Kodali, and D. Srivastava, Chem. Rev. **96**, 1327 (1996), and references therein.
[19] A. Nordsieck, Math. Comput. **16**, 22 (1962).
[20] D. W. Noid, M. L. Koszykowski, and R. A. Marcus, J. Chem. Phys. **67**, 404 (1977).
[21] B. J. Min, Y. H. Lee, C. Z. Wang, C. T. Chan, and K. M. Ho, Phys. Rev. B **46**, 9677 (1992).
[22] Y. J. Chabal, A. L. Harris, K. Raghavachari, and J. C. Tully, Int. J. Mod. Phys. B **7**, 1031 (1993).
[23] J. C. Tully, Y. J. Chabal, K. Raghavachari, J. M. Bowman, and R. R. Lucchese, Phys. Rev. B **31**, 1184 (1985).
[24] L. V. Zhigilei, D. Srivastava, and B. J. Garrison, Surf. Sci. (to be published).
[25] P. Guyot-Sionnest, P. H. Lin, and E. M. Hiller, J. Chem. Phys. **102**, 4269 (1995).
[26] Y.-C. Sun, H. Gai, and G. A. Voth, J. Chem. Phys. **100**, 3247 (1994).
[27] N. L. Allinger, Y. H. Yuh, and J.-H. Lii, J. Am. Chem. Soc. **111**, 8551 (1989). We developed our own code for MD simulations of hydrocarbon systems using this reference. Equations (1) and (2), however, have errors which were corrected through private discussions with N. L. Allinger. The accuracy of our code was checked by computing and comparing the force constants and vibrational frequencies of a few hydrocarbon molecules with the standard MM3-92 code, commercially available from QCPE, University of Indiana, Bloomington, IN 47405.
[28] A. DeVita, G. Galli, A. Canning, and R. Car, Nature **379**, 523 (1996).
[29] S.-T. Lee and G. Apai, Phys. Rev. B **48**, 2684 (1993).
[30] J. C. Angus, A. Argoitia, R. Gat, Z. Li, M. Sunkara, L. Wang, and Y. Wang, in *Thin Film Diamond* (Ref. 2), p. 1.
[31] C. Wild, R. Kohl, N. Herres, W. Müller-Sebert, and P. Koidl, Diamond Relat. Mater. **3**, 373 (1994).
[32] B. E. Williams, J. T. Glass, R. F. Davis, K. Kobashi, and K. L. More, in *Proceedings of the First International Symposium on Diamond and Diamond-like Films*, edited by J. P. Dismukes (Electrochemical Society, New York, 1989), p. 202.
[33] K. E. Spear and M. Frenklach, in *Synthetic Diamond: Emerging CVD Science and Technology*, edited by K. E. Spear and J. P. Dismukes (Electrochemical Society, New York, 1994), p. 243.